

HEAVY ION RECIRCULATING INDUCTION LINAC STUDIES

TERRY F. GODLOVE

FM Technologies, Inc., Fairfax, VA 22032.

(Received 3 December 1990).

A high-current, heavy-ion accelerator is now recognized as a leading contender for a driver for inertial fusion power plants. The cost of an induction linac driver for a 1-GWe plant is likely to be about \$1 billion. A multi-beam recirculating induction linac, while introducing serious new issues, could significantly reduce the cost. In this paper, some initial studies by a group at the Lawrence Livermore National Laboratory with representatives from the Lawrence Berkeley Laboratory, and by F. M. Mako and myself at FMT, are reviewed. Initial effort indicates that the following approximate parameters are appropriate: cycle time ≈ 3 ms; 4 to 8 beamlets; and circumference ≈ 3 km. Transport stability is required for ≈ 50 turns. While fewer quadrupoles and cavities are needed, a large number of pulsed dipoles (with consequent losses) and programmed, multi-pulsed accelerating cavities are necessary. Apertures, lattices and losses are calculated based on assumed quadrupole strength and beam parameters. Parameter tradeoffs are illustrated with examples.

1 INTRODUCTION

A principal cost element in inertial fusion is the driver—the laser or accelerator that provides intense beams of light or particles to compress and heat a thermonuclear fuel pellet to ignition. U.S. heavy ion researchers, principally at the Lawrence Berkeley Laboratory (LBL), have concentrated their efforts on induction linac drivers¹.

A major Heavy Ion Fusion Systems Assessment (HIFSA) was completed for the U.S. program in 1986². The HIFSA study concluded that an induction linac driver for a 1-GWe plant would cost between \$0.6 and \$1.2 billion, depending on several key assumptions in the design. While these costs are not out of line with other fusion system estimates, nevertheless there is a strong incentive to reduce costs, not only for a fusion driver, but also for experimental research facilities to develop such drivers.

One cost reduction approach has been adopted in HIF designs for some years, namely the use of multiple beams to achieve the required kiloampere beam currents. Current LBL designs employ 16 “beamlets” (the term refers to a compact array of separate beams) in the main induction linac, while as many as 64 beamlets may be required at the ion source. Each beamlet must have separate focusing elements, but the entire array is carried through the high-voltage induction cores. The total cost is then much less than would be the case if separate cores were required. The LBL group has conducted extensive research on multiple beams, culminating in the successful operation of the Multiple Beam Experiment (MBE-4), which employs four beamlets³.

A recirculating linac represents a logical, albeit more complex, next step. Why not direct the beams back through the same cavities to cut costs? In late 1984 I submitted a brief note on this subject to the HIFSA study participants. The limited scope for the HIFSA precluded its inclusion as a major study element. It now seems timely to examine the concept in more detail.

A prime example of a recirculation design is the Continuous Electron Beam Accelerator Facility (CEBAF) at Newport News, VA, now under construction⁴. The design employs four turns, expandable to six, in a racetrack configuration. A 500-MeV, superconducting rf linac is placed in each straight section of the racetrack, yielding 4 GeV for four turns. While CEBAF is for relativistic electrons, and is designed for a continuous beam rather than intense pulses, nevertheless the cost savings inherent in recirculation are indisputable.

The primary thrust of this review is to describe some results from a program, RECIRC, written to calculate parameters pertinent to a recirculating induction linac. Conceptual design is done at an intermediate level. Envelope equations are used for the beam radius, and accelerator components are calculated on the basis of scaled models. The program is fast (≈ 1 s) and convenient, allowing a quick look at a variety of parameter variations. Currently the input consists of more than 25 independent parameters. The approach is similar to that used by the McDonnell-Douglas team for the HIFSA study².

The principal assumption, and technical issue, is beam stability. The beam is treated as if it were in a long linac with the length equal to the circumference times the number of turns. The quadrupole strength is held constant at the maximum available level throughout the acceleration cycle. This allows much higher beam currents than would be the case if the quads were ramped from a low level in synchronism with the dipoles, as they are in a normal synchrotron. The quadrupoles may be either super-conducting or conventional. If normal, they would doubtless be pulsed to reduce power consumption, provided the pulse is reasonably flat during the acceleration cycle.

Recently, the development of RECIRC has been parallel to, and has benefited from, a recirculator study project undertaken at the Lawrence Livermore National Laboratory (LLNL) assisted by staff members from LBL. I will include some of their work. Other papers in these proceedings give details.

Low energy injection is an issue for a recirculator as well as a linac, primarily because allowed beam currents are greatly reduced at low energy. Injector systems must use more beams followed by merging, or use longer pulses, or both. In most examples described in Section 3, I use an energy ratio of 14 in each of two recirculators, starting with a 50-MeV, 32-beam linac with 4:1 merging. The LLNL group is studying systems based on four recirculators, starting with 2-MeV injection.

2 DESCRIPTION OF PROGRAM

The same generic lattice, shown in Figure 1, is used throughout the accelerator. Quadrupoles and short vacuum/diagnostic sections are assumed in every lattice. The

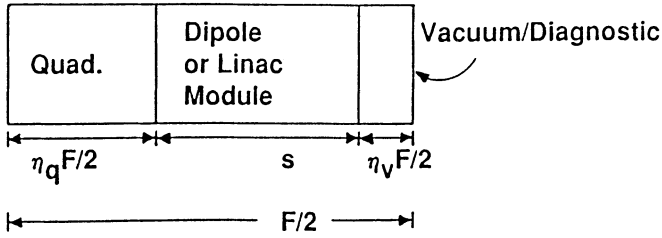


FIGURE 1 Generic half-lattice used throughout the circumference. The same length, s , is used for a dipole or an accelerating module. η_q and η_v are the fraction of the circumference (or lattice) required for quadrupoles and vacuum/diagnostic equipment, respectively.

remaining length, designated s in Figure 1, refers to either an accelerating module, or dipole, or space allowed for injection and extraction. Occupation fractions are assigned to these components *relative to the circumference*.

This method allows the program to be independent of the accelerator configuration. It applies to a racetrack or a multi-sided polygon. Put another way, a given portion of the circumference may contain a series of dipoles in module s , or a series of accelerating cavities, or any arbitrary sequence of the two. Two restrictions are implied by this method: (1) every lattice contains the same quad and vacuum/diagnostic lengths; and (2) the length of the dipoles and the accelerating modules are assumed to be equal. These restrictions are not considered serious at this stage of study.

All lengths are either chosen as independent parameters (by choosing occupation fractions) or are calculated in a self-consistent way based on beam physics parameters and required energy per turn. Exceptions to the “independence” of a few parameters are noted as the description proceeds.

The number of turns, N , required to achieve the assumed final energy is calculated in a turn-by-turn integration. The integration step is varied from a quarter-turn at injection to a full turn for the last half of the cycle. If the resulting number of turns is not desired, the program is rerun with a different dipole rise time, T . MKS units are used throughout.

2.1 Dipole Waveform

Two options for the pulse waveform applied to the dipoles are calculated simultaneously in RECIRC. These are shown in Figure 2 and detailed as follows:

(a) *Sine Wave*:
$$B/B_m = \beta\gamma/(\beta\gamma)_m = \sin(\pi t/2T), \tag{1}$$

where $B(B_m)$ is the dipole (maximum) magnetic field, $\gamma = 1 + (E/Mc^2)$, $\beta = (1 - \gamma^{-2})^{1/2}$, E is the kinetic energy, M the ion mass, c the velocity of light, and T is the quarter-period rise time of the dipole field. B_i , B_f are the initial and final field values for the initial and final kinetic energy, E_i and E_f , respectively. Similarly, t_i and t_f are the time at injection and extraction ($t = 0$ at $B = 0$). The

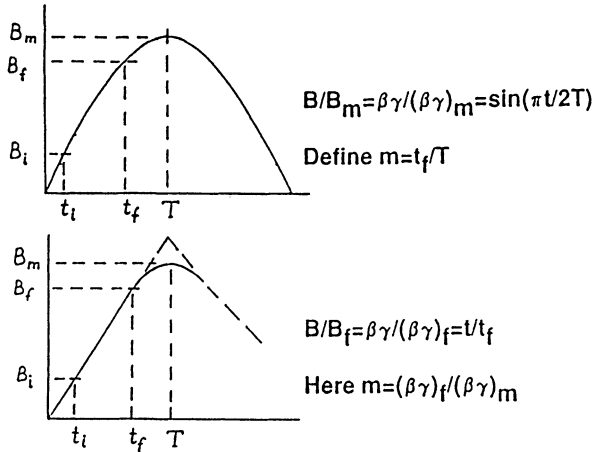


FIGURE 2 Dipole magnetic field vs. time for the two options considered for the dipole waveform: (a) sine wave, and (b) linear.

maximum value of $\beta\gamma$, needed for calculation purposes only, is given by

$$(\beta\gamma)_m = (\beta\gamma)_f B_m / B_f. \tag{2}$$

A separate independent parameter, m , is defined as the fraction of the rise time from $t = 0$ to $t = t_f$. That is, $m = t_f / T$. A value of m around 0.8 appears to be optimum. Larger values suffer from reduced energy gain per turn near $t = T$, while smaller values do not take advantage of the available dipole field. In our examples, $m = 0.85$ and $(t_f - t_i) / T$ is typically $\simeq 0.67$.

The time at injection, t_i , is required later. It is

$$t_i = (2T/\pi) \sin^{-1}(B_i/B_m), \tag{3}$$

where $B_i = B_f(\beta\gamma)_i / (\beta\gamma)_f$.

(b) *Linear Waveform:* In this option we use a model which places the physical maximum field, B_m , midway between B_f and the peak of a fictitious triangular waveform, as shown in Figure 2(b). This is done so that the physical value of B_m can be used as input for both options. Thus the mathematical peak is at $B = B_m(3 - m)/2 = B_f/m$. In this model the maximum value of $\beta\gamma$ is

$$(\beta\gamma)_m = (\beta\gamma)_f / m \tag{4}$$

and

$$t_f = mT, \quad t_i = T(\beta\gamma)_i / (\beta\gamma)_m \tag{5}$$

Option (a), the sine wave, applies to a capacitor discharge circuit for the dipoles. However, a major disadvantage is the resulting large variation in the accelerating voltage per turn. For example, for $E_f/E_i = 10$ to 15, the energy per turn varies by a factor up to 4:1. This variation can be accomplished by not pulsing a gradually increasing number of cavities, but it is less efficient than fully utilized cavities.

The linear waveform option features a constant energy per turn, except for a small relativistic effect, and is thus much more efficient in the use of cores. However, the circuits required to generate a linear waveform are more complex, and would require some electronic engineering studies. Perhaps a compromise between these two extremes might be feasible. The addition of only one or two harmonics to the fundamental sine wave, for example, might yield a quasi-linear waveform at modest increase in dipole pulser cost. The added cost may be more than offset by other reductions. In one case described in Section 3, 60% more Metglas is required for the sine-wave option. In either option, the energy per turn must be controlled, either by amplitude control of the cavity pulsers or, perhaps more easily, by control of the number of cavities energized per turn.

RECIRC calculates both waveform options using separate turn-by-turn integration. The option desired is chosen before the parameter adjustments are made to achieve self-consistency. The choice of B_m is a separate consideration. Dipole losses are a strong function of maximum field and must be traded off with system size.

2.2 Input Parameters

Input parameters are divided into five groups: system, dipoles, beam physics, induction cores, and circumference occupation fractions. Although the circumference, S , and the accelerator module occupation, η_a , are used as input parameters, they must in fact be iterated to achieve a self-consistent design. η_a is adjusted to match the required energy gain in the first turn, and S is varied to match the required total dipole length. In addition, the quadrupole occupation, η_q , must be consistent with the beam parameters. The five circumference occupation fractions sum to unity. The dipole fraction is picked to be the dependent variable, since it has the fewest restrictions. It is obtained from $\eta_d = 1 - \eta_q - \eta_a - \eta_v - \eta_i$.

An important system parameter to be optimized is the number of beamlets, b . This parameter, together with the physical separation between beamlets, determines the size and weight of the Metglas accelerating cores which surround the beamlets⁵. Currently, the program calculates the separation between beamlets, and the size weight of the core material, based on the dipole dimensions, for 1, 4, and 8 beamlets. The geometry for 4 beamlets is shown in Figure 3.

The input beam parameters include the beamlet electrical current, I , the mean beamlet radius, a , the beamlet clearance factor, $C_f = \text{aperture}/\text{mean beamlet radius}$, the quadrupole tip field, and the zero-current phase shift per lattice period, σ_0 . For the examples of Section 3, σ_0 is fixed at 81 degrees¹. The beam edge field, B_q , is the tip field divided by the clearance factor.

2.3 Beam Formulas

The beam formulas are taken from the review by Lee⁶. The lattice period, F , is given by

$$F = 2(aBR\sigma_0/\eta_q B_q)^{1/2}, \quad (6)$$

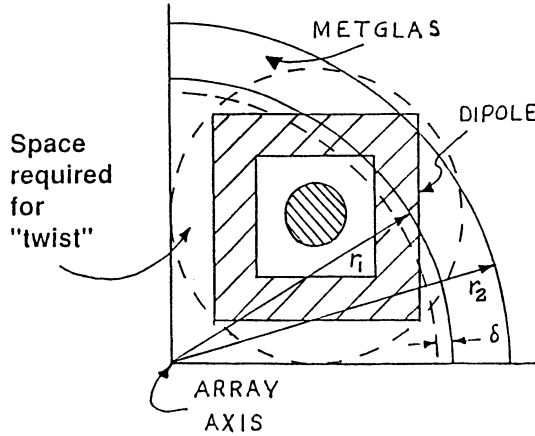


FIGURE 3 Beamlet geometry for a four-beamlet array. The dashed circle represents the space required to "twist" the beams gradually around the array axis. r_1 and r_2 are used to calculate the cross-sectional area of Metglas core material.

where $BR = 3.13(\beta\gamma)_i A/Q$ at injection. The linac module (and dipole) length, s , is then:

$$s = (1 - \eta_q - \eta_v)F/2. \tag{7}$$

The beam phase shift, σ , depressed by space charge, is

$$\sigma = \{\sigma_0^2 - 2 \times 10^{-7}(I/BR)(F/\beta\gamma a)^2\}^{1/2} \tag{8}$$

using the parameters at injection. Finally, the normalized emittance is

$$\varepsilon = \sigma\beta\gamma a^2/F. \tag{9}$$

For a high-energy ring the normalized emittance is fixed by the requirements for final focus, and is typically $\simeq 8$ mm-mrad. Thus a , I , and η_q must be iterated to yield the desired emittance. To speed this iteration a separate calculation of η_q is made as follows:

$$\eta_q = 4\{(\varepsilon/a)^2 BR + 2 \times 10^{-7}I\}/a\sigma_0(\beta\gamma)^2 B_q.$$

This value of η_q is then used as a revised input parameter.

Equations (6), (7) and (9) yield identical results when final extraction parameters are used, but the phase shift formulas change as follows, for fixed quadrupole strength and beam current:

$$(\sigma_0)_f = (\sigma_0)_i(\beta\gamma)_i/(\beta\gamma)_f$$

and

$$\sigma_f = \{\Phi^2 + (\sigma_0)_f^2\}^{1/2} - \Phi,$$

where $\Phi = 10^{-7}IF/\varepsilon(\beta\gamma)_f(BR)_f$.

2.4 Matching Linac and Dipole Occupations

The average energy during the first turn, $(E_1)_{ave}$, based solely on the assumed energy gain parameters, is $(E_1)_{ave} = E_i + QS\eta_a(dV/dz)/2$. From this, the average velocity is calculated and used to compute the first turn travel time which, added to t_i in Eq. (3) or Eq. (4), gives the time, t_1 , at the end of the first turn. This is used to calculate the required $\beta\gamma$ based on the assumed time variation of the dipole field. For the sine-wave $(\beta\gamma)_1 = (\beta\gamma)_m \sin(\pi t_1/2T)$, and for the linear case $(\beta\gamma)_1 = (\beta\gamma)_m t_1/T$.

From these values we obtain the energy *required* after one turn. This value is compared with $E_1 = E_i + QS\eta_a(dV/dz)$, and η_a is iterated to achieve a match. In other words, we match the energy gain due to the cavities with the energy gain required by the rising dipole field. The result of course depends on which of the two waveform options one chooses.

After finding an acceptable energy match, the computed dipole occupancy, η_d , will not in general equal the value calculated from $2\pi R/S$. These two values are compared and S adjusted to achieve a final result.

2.5 Model Dipole and Quadrupole

Superconducting dipoles are ruled out because of the fast cycle time. An air-core magnet is possible in principle, but a conventional pulsed iron magnet operating below the saturation limit, ≈ 1.8 T, is the clear choice on the basis of stored energy and power dissipation. The dipole formulas, based on the model of Figure 4, are summarized here.

The gap height, width, and length are d , w , and s , respectively. The iron is laminated with thickness, f , and n turns of copper are used with height, h , and thickness, x . The thickness of the laminations and the copper are adjusted to keep the dipole losses within limits, typically 7–12% of the dipole stored energy. The thickness of iron

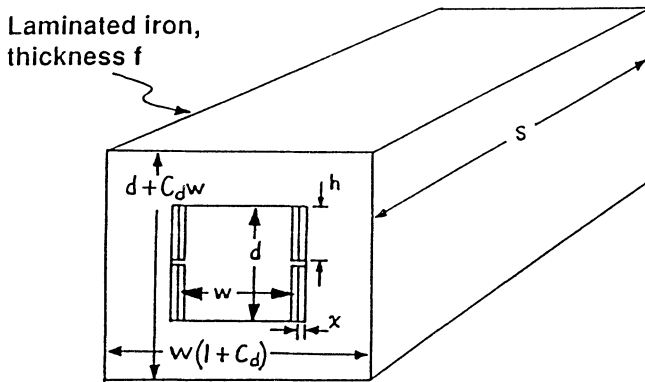


FIGURE 4 Model dipole. The thickness of iron around the gap is $C_d w/2$, where w is the gap width and C_d is a correction factor near unity. Four turns of copper wire are illustrated. The iron is laminated with thickness f .

around the gap is $wC_d/2$, where C_d is a correction factor to account for the fact that a realistic magnet requires more iron than the ideal, $w/2$. Pending more precise design calculations we have arbitrarily set $C_d = 1.25$.

The inductance is given by $L = \mu_0 n^2 w s / d$, provided $\mu_m \gg 1$ and $\mu_m d / p \gg 1$, where p is the magnetic flux path length and μ_m is the iron permeability. The resistance is $r = 2n(s + w) / h x j_{cu}$, where j_{cu} is the conductivity of copper.

The peak current is $i = dB_m / n \mu_0$. The stored energy is $W_s = (1/2) Li^2$.

The required capacitance, for a quarter-period, T , is $(2T/\pi)^2 / L$, and the peak voltage is $\pi i L / 2T$. The volume of iron is $V_{fe} = s w C_d (w + w C_d + d + n x)$, and the weight is $7870 V_{fe}$.

The energy loss per dipole per pulse is calculated for all four types of dipole losses. Average power is based on the computed number of dipoles and the input repetition rate. The losses are:

1) coil resistive loss $= i^2 r T$, assuming the circuit is designed to recover the stored energy in a half-cycle ($2T$) rather than a full cycle:

2) coil eddy current loss $= (\pi B_m)^2 x^3 n h s j_{cr} / 24 T$:

3) core eddy current loss $= (\pi f B_m)^2 V_{fe} j_{fe} / 48 T$: and

4) hysteresis loss $\simeq 1000 V_{fe}$, at 1.6 tesla.

The copper wire and lamination parameters are chosen primarily for low losses. It is assumed that the required voltage can be split between several modular circuits. An example dipole very close in both size and required pulse length to that required here is described by Pearce *et al.*⁷

The quadrupole, shown in Figure 5, is taken from a review by Fischer⁸. The area of iron and copper are $10.6d^2$ and $0.90d^2$, respectively, and the overall width is $4.0d$, where d is the aperture, assumed identical to the dipole aperture. The required ampere-turns is dB_{tip} / μ_0 , including all four poles. The length is computed using Eq. (6), and is $\eta_q F / 2$.

Iron area = $10.6 d^2$
 Copper area = $0.90 d^2$
 Width = $4.0 d$
 ni/pole = $dB_{tip} / 4 \mu_0$

(MKS units)

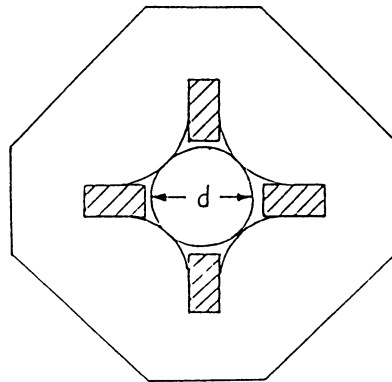


FIGURE 5 Model quadrupole, from Ref. 8.

In the summary calculations, the total weight of iron is used as a figure of merit of the system. Copper weight is typically 10% that of iron.

2.6 Accelerator Modules

Figure 3 shows the geometry used for calculating the amount of core material in the accelerating cavities for four beamlets. As noted above, the length of each accelerating module is identical to the length, s , of each dipole; what is needed are the radii of the cores.

The geometry shown in Figure 3 allows enough space between dipoles to rotate them about their own axes in order to “peel” the beamlets in and out along radial lines for injection and extraction. It also allows space to slowly rotate the entire array about the array axis while maintaining the vertical orientation of the magnetic field. This type of beamlet “twisting” would be a relatively simple way to equalize the path length of each beamlet. The required space is defined by the dashed circle around the dipole. This geometry thus determines the desired radii and the separation between dipoles.

The inner radius, r_1 , is given by $r_1 = w(1 + C_d) + aC_r + \delta$, where C_d is the dipole iron “realism” factor, C_r is the beamlet clearance factor, and δ is the radial thickness of wall material needed to contain the Metglas. The outer radius is then $r_2 = r_1 + (u/\Delta BC_p)(dV/dz)$, where u is the pulse duration, C_p is the packing fraction of the core material, ΔB is the total magnetic field swing, and dV/dz is the average electric field in the module. The volume and weight of the Metglas is then calculated. In the examples described in Section 3 the values $C_p = 0.8$, $\Delta B = 2.5$ Tesla and $\delta = 1$ cm are used.

The above formulas are included in RECIRC for 1-, 4-, and 8-beamlet arrays using formulas similar to those above for four beamlets. The formulas for one beamlet are included so that comparisons can be made with multiple-beam arrays based on separate accelerating cavities.

The geometry of Figure 3 is not necessarily optimum. A major alternative is to arrange the dipoles in a close-packed array, eliminating the spacing shown. This would have the distinct advantage of reducing the amount of core material. However, the injection/extraction geometry and the path equalization would have to be solved in a different way. For example, “peeling” in a close-packed array can be done in the vertical and horizontal planes at different, but nearby, locations along the axis. Path equalization might be accomplished by periodically peeling the beamlets out just far enough to allow the dipoles to be slowly twisted about the array axis. The size of the array would then be close-packed through the linac regions and separated as in Figure 3 through the bending/twisting regions. The number of such shifts between a close-packed array and a spread array would have to be optimized and, in particular, would depend on the distance allowed between linac sections before undue longitudinal spreading takes place due to space charge.

In this review we adopt the conservative position that the dipoles should be spread throughout the recirculator as shown in Figure 3. If the dipoles are close-packed, the required amount of Metglas is somewhat reduced.

2.7 Longitudinal Stability

A formula due to Lee is included in RECIRC to give a relative indication of the longitudinal resistive wall instability⁹. The gain, G_i , which occurs in the exponent, is as follows:

$$G_i = 5.7 \times 10^6 (E_f - E_i) (Z_{\text{cell}}/Z_{\text{beam}}) \mu \beta^2 / NISH, \quad (10)$$

where $H = 0.5 + 2 \ln(d/2a)$ is a geometry factor, Z_{cell} is the impedance of the accelerating cell, Z_{beam} is the ratio of the cell voltage to total current (bI), and the other symbols have been defined. In the examples that follow I have used $Z_{\text{cell}}/Z_{\text{beam}} = 0.13$ and $H = 1.44$. However, this formula does not include capacitance. The theory has been recently reexamined by Lee and Smith who find reduced growth rates¹⁰. Pending further analysis we use Eq. (10) only as a relative index. Lee and Smith also point out that it should be possible to control the instability with a “feed-forward” system.

3.0 EXAMPLE DESIGNS

The main purpose of the program at this stage is to illustrate tradeoffs of major parameters. Table 1 gives most of the key input parameters and computed results for seven examples of the high energy ring in a power plant design. The input values chosen conform to past studies: $E_f = 10$ GeV, $W_s = 4$ MJ, and the repetition rate is 10 Hz. A normalized emittance of 8 mm-mrad is chosen to conform to most studies of the final focus. The ratio of aperture to mean beam radius is fixed at 1.6. Beam currents are chosen to give a total peak beam power of 8–10 TW at extraction (based on injected beam current). Additional bunching is required in the recirculator itself, perhaps during the last few turns, and also in the transport line between the recirculator and the target, to achieve 150–200 TW on target.

The number of recirculated turns, fixed at $N = 50$, is somewhat arbitrary at this stage. Further study is required to determine the impact of this number on beam physics difficulties as well as the point of diminishing returns on system cost. The injection energy is another system variable. Higher energy allows larger injected current but requires a larger injector system. The LLNL group uses injection at 1 GeV based on a series of staged recirculators. I have used 700-MeV injection based on a scenario of two recirculators plus a 50-MeV linac injector with 4:1 merging before injection into the first ring. Example 7 uses 1 GeV for comparison.

The pulsed dipole parameters are chosen to minimize loss, which, in these examples, is typically 10% of the stored energy. Loss increases rapidly with aperture, hence with beam radius, and is sensitive to the copper thickness, typically $\simeq 2$ mm. The iron lamination is normally $\simeq 1$ mm thick. Fortunately, the average current density in the coils is low enough at 10 Hz rate that water cooling interior to the copper wire should be unnecessary.

The electric field assumed for the accelerating modules, $dV/dz = 0.6$ MV/m, refers to the average field over the module of length s . The field in the gaps is higher,

TABLE 1
Example Designs

Case	1	2	3	4	5	6	7
Dipole Waveform	Lin.	Sine	Lin.	Lin.	Lin.	Lin.	Lin.
Beamlet Current I (A)	250	250	200	200	100	200	250
No. of Beamlets b	4	4	4	4	8	8	4
Mass A (amu)	200	200	150	150	150	150	150
Charge State Q	1	1	1	1	1	2	1
Beam radius a (cm)	4.0	4.0	2.9	2.9	2.0	2.8	3.0
Dipole Field B_m (T)	1.0	1.0	1.0	1.6	0.8	0.8	1.0
Quadrupole Tip Field (T)	4.0	4.0	1.7	1.7	1.7	1.7	1.7
Quadrupole Occupancy η_q	0.20	0.20	0.40	0.40	0.37	0.40	0.34
Linac Occupancy η_a	0.118	0.168	0.090	0.128	0.080	0.075	0.101
Circumference S (m)	2604	2890	3430	2416	3800	2050	2962
Lattice Length F (cm)	4.97	4.97	4.25	4.25	3.69	2.96	5.21
Rise Time T (msec)	3.45	3.17	3.94	2.77	4.36	2.35	3.51
Pulse Durat. u (μ s)	0.40	0.40	0.50	0.50	0.50	0.50	0.40
Peak Pwr $IE_f b/Q$ (TW)	10.0	10.0	8.0	8.0	8.0	8.0	10.0
Metglas Weight (Gg)	1.9	3.1	2.0	2.0	4.6	3.0	1.6
Iron Weight (Gg)	6.7	7.0	5.9	4.0	6.7	6.5	5.0
Dipole Energy (MJ)	34.9	34.9	16.0	25.5	12.1	11.9	17.1
Dipole Power (MW)	31.2	31.1	19.1	23.7	20.5	14.0	19.2
Longitudinal instability (Rel.)	5.6	5.1	9.1	13.0	15.8	15.1	6.5

Notes: All cases have $E_i = 0.7$ GeV (except Cases 7, which has $E_i = 1$ GeV); $E_f = 10$ GeV; $dV/dz = 0.6$ MV/m; $W_s = 4$ MJ; rep. rate = 10 Hz; $\eta_i = 0.09$; $\eta_o = 0.08$; $\sigma_o = 81$ deg; $\epsilon = 8$ μ rad; $C_d = 1.25$; $C_f = 1.6$; $m = 0.85$; and $N = 50$ turns. I , a and u are given at injection. The total peak beam power at extraction does not include bunching in the recirculator. Iron weight includes dipoles and quadrupoles.

depending on detailed design, and the field averaged over the circumference is much lower, specifically $\eta_a(dV/dz)$.

Room-temperature, pulsed quadrupoles are assumed for all of the examples except the first two. Superconducting quad's are being studied by the LLNL group and, if the geometry is feasible, have a definite advantage. Quadrupole losses are not yet included in RECIRC.

The first two examples illustrate the use of superconducting quad's (tip field 4 tesla) as well as the difference between the linear and the sine-wave dipole option. The dipole maximum field has been set at 1 tesla to reduce losses; otherwise they would be much higher with a 4 cm beam radius. The sine wave option causes a slightly larger circumference, but the primary effect is 60% more Metglas.

Case 3 illustrates the use of room temperature quadrupoles (tip field 1.7 T) and the advantage of a smaller beam radius, 2.9 cm. This is compensated by doubling the quadrupole occupancy, from 20% to 40%, and by reducing the ion mass to 150. The result is a substantial reduction in dipole stored energy and power. The disadvantage is a reduction in beam power by 20% and a somewhat worse instability index. Whether the reduction in mass has a serious effect on target performance can only be answered by more comprehensive studies (and eventually only by experiment).

In Case 4 the dipole maximum field has been increased to 1.6 tesla for direct

comparison with Case 3. Other input parameters remain identical. Although the circumference is considerably smaller, the substantial increase in dipole energy and power is evident.

Case 5 illustrates doubling the number of beamlets, and in Case 6 the ion charge state is also doubled. In both cases the dipole field is further reduced to 0.8 T to reduce losses. The beam power is maintained at 8 TW by adjusting the beamlet current and quadrupole occupancy. Case 6 is especially interesting because it has the lowest stored energy and dipole power in the Table. However, the instability index for both cases is highest.

Case 7 is included as an example of using an injection energy of 1 GeV. The beam power is restored to 10 TW; otherwise it is generally similar to Case 3.

RECIRC runs for the injector ring (50 to 700 MeV) give the following results for $A = 150$, 8 beamlets, $Q = 2$, $I = 11$ A, $B_q = 1.7$ T, $B_m = 1$ T, the linear waveform, and a reduced module field strength, $dV/dz = 0.1$ MV/m:

$$a = 3 \text{ cm,}$$

$$\eta_q = 0.33,$$

$$\eta_a = 0.088,$$

$$S = 432 \text{ m, and}$$

$$T = 1.85 \text{ msec.}$$

The beam pulse duration is much longer ($u = 9.1 \mu\text{sec}$) leading to a Metglas weight of 5.5 Gg. The iron weight is 1.4 Gg, the dipole stored energy 4.4 MJ, and the dipole power is 4.3 MW. The calculated instability index is an ominous 127. In this scenario a bunching factor of four is required in the recirculator and another factor of 4.5 is required between the two recirculators.

6 SUMMARY AND OTHER ISSUES

A fast, convenient code has been written to accommodate the large number of parameters involved in the conceptual design of a high-current, heavy-ion, recirculating induction linac. Dipoles, quadrupoles and linac cavities are included using scaled models, in a framework which is independent of the details of the configuration and allows a broad parameter study. Using the code, several 10-GeV recirculator example designs are given which provide adequate beam current and appear to be reasonable in terms of total component weight and power losses. Cost algorithms have not yet been added to RECIRC.

The designs show the effect of changes in key parameters. For example, dipole energy and power losses increase rapidly as the beam radius is increased from 2 cm to 4 cm to provide more beam current. Designs based on charge state two and mass 150 exhibit low stored energy and dipole power, but the calculated longitudinal instability index is worse.

A great deal of work remains. Emittance growth issues as well as stability issues must be studied both theoretically and experimentally. Vacuum chamber walls must

tolerate the pulsed magnetic fields without undue losses. The LLNL group is making progress in costing its 4-ring conceptual design, and has studied injection/extraction schemes, superconducting quadrupoles, vacuum requirements, and high-power pulser issues. Given success in stability and emittance control, these designs have the potential for a substantial reduction in the cost of a heavy-ion inertial fusion driver.

7 ACKNOWLEDGEMENTS

I am indebted to the LLNL group, especially D. Hewett, who assisted with RECIRC and reviewed the manuscript, and to S. Yu, J. Barnard and L. Reginato for several discussions. F. M. Mako provided the design equations for the pulsed dipoles. An early portion of this work was supported by a Phase I grant in the Small Business Innovation Research program of the U.S. Department of Energy.

REFERENCES

1. Denis Keefe, AIP Conf. Proc. **152**, 63 (1986).
2. Fusion Technology **13**, 189–396 (1988); also HIFSA articles in Ref. 1.
3. T. J. Fessenden, *Nucl. Instrum. Meth.* **A278**, 13 (1989).
4. H. A. Grunder *et al.* IEEE Cat. 87CH2387-9, 13 (1987).
5. Metglas is a trade name of Allied-Signal, Inc.
6. E. P. Lee, AIP Conf. Proc. **152**, 461 (1986).
7. P. Pearce *et al.* IEEE Trans. Nucl. Sci. **NS-32**, 3613 (1985).
8. G. E. Fischer, AIP Conf. Proc. **153**, 1132 (1987).
9. Eq. (10) is the form used by the LLNL group, and derives from E. P. Lee, Proc. 1981 Linear Accel. Conf., Los Alamos Report LA-9234-C, p. 263.
10. E. P. Lee and L. Smith, "Asymptotic Analysis of the Longitudinal Instability of a Heavy Ion Induction Linac," Proc. 1990 Linear Accel. Conf.